Synthesis and Evaluation of Titanium Oxide Modified Mussel Inspired Nanoparticles for Synergetic Photothermal and Photodynamic Effect

Nahla Rahoui[1a], Pei Zhou[1], Nadia Taloub[1], Mohammad Hegazy[1] and Yu Dong Huang[1b]

[1]MIIT Key Laboratory of Critical Materials Technology for New Energy Conversion and Storage, School of Chemistry and Chemical Engineering, Harbin Institute of Technology, P. O. Box: 1254, Harbin 150001, People's Republic of China.

E-mail: [a]nahlarahoui@hit.edu.cn; [b]huangyd@hit.edu.cn.

Abstract. Applying two therapeutical modality using one system is primordial for enhanced treatment efficiency and decreased side effects. The main objective of this work was to develop polydopamine (PDA) based hybrid nanoparticles with strong near infrared absorbance and good NIR to heat conversion efficiency. The results proved successful preparation of polydopamine nanoparticles (PDNS) decorated with metal oxide (TiO_2), spherical shaped of ~268 nm mean diameter and negative surface charge (ζ=−16.40 mV). The prepared PDNS@TiO_2 were characterized by FT-IR, UV-Vis, TEM and XPS. They exhibit a good thermal stability and significant photothermal conversion efficiency (η=34.9%). On other hand ESR spectra proves the ability of this kind of nanostructures to generate of ROS under UV irradiation due to the presence of TiO_2 on the surface. This paper describes the design and evaluation of novel nanostructures for combined photothermal and photodynamic effect. A remarkable synergistic therapeutic effect has been achieved compared with respective single treatments. This work suggests that the PDA-based nanoplatform can be a universal scaffold for single or combined therapy.

1. Introduction

The photothermal therapy (PTT) is considered as very promising tool to induce selective therapeutic effect by malignant tissues ablation. The main step in design of any PTT nanostructures is the selection of high absorptive agent in the NIR region. At the same time safe and efficient PTT agent [1]. The mussel inspired polydopamine polymer as NIR photothermal agent is known of its ease, durable deposition on all types of solid interface inorganic and organic substrates at different controllable thickness and remarkably high stability, thus PDA have been used as a versatile tool for surface modification and coating [2, 3].

The PDA was considered as a versatile material for surface modification due to its abundant amine cationic groups and also phenolic anionic groups known as indole, catechol, quinone and indolic/catecholic [3] that enhance metal ion chelation and the reducive effect of PDA on any metallic cations [4]. Besides the high photo-stability, PDA provides a high photo-protection effect to the coated material. Meanwhile PDA can absorb well in the NIR region and convert it into heat, especially PDA nanoparticles (PDNS) that have a high conversion efficiency of 40%. [5-7] To increase the therapeutic effect of the synthesised system and to get a combination of photothermal therapy and photodynamic

Content from this work may be used under the terms of the Creative Commons Attribution 3.0 licence. Any further distribution of this work must maintain attribution to the author(s) and the title of the work, journal citation and DOI.
Published under licence by IOP Publishing Ltd

therapy, PDNS could be decorated with TiO_2 nanoparticles using LPD method. The use of hybrid nanomaterials for combined therapeutic effect is more promising for NIR induced photothermal conversion efficiency through PDNS and UV induced generation of reactive oxygen species (ROS) to reduce the toxicity effect of metallic nanoparticles on normal tissues by the way limits the undesirable side effects [1,8]. Several studies investigated the titanium dioxide (TiO_2) as therapeutic agent, it has distinct properties such as: it low cost, structural stability, optical properties including high ultraviolet absorption, visible light induced photo-oxidation, remarkable photo-stability, good biocompatibility (widely used as food e.g., jelly, gum, food, excipient in medicine, toothpaste and cosmetics) [9, 10] besides the wide environmental application as photocatalysts for water, air, and soil decontamination [10]. Recently, the application of TiO_2 as photo absorbing agents that absorb well in the UV region ($\lambda = 275–390$ nm) at the same time can generate a cytotoxic ROS reactive oxygen species or free radicals (e.g. hydroxyl and superoxide radicals) [11].

In this work, in order to have an enhanced NIR photothermal therapeutic effect, PDNS and TiO_2 have been incorporated into one system (see figure 1) by design of PDNS interface with TiO_2 after chelation of Ti^{4+}, nucleation and growth through PDNS catechol groups [12]. The system have been characterised by several methods to prove successful synthesis. The photothermal measurements reveals the enhanced of photothermal conversion efficiency of TiO_2 designed PDNSs compared to unmodified PDNS besides the further generation of ROS after UV irradiation.

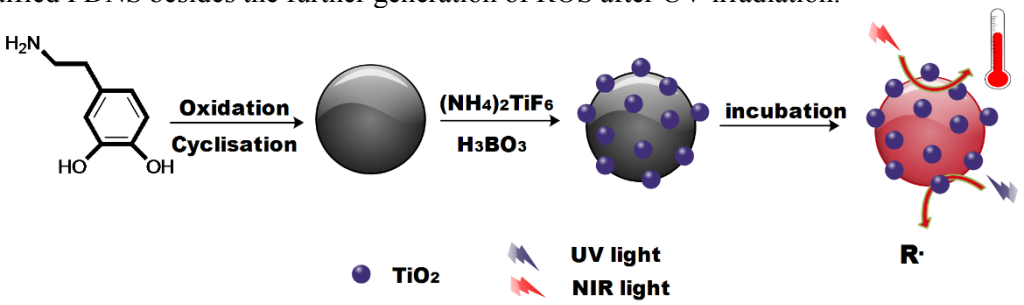


Figure 1. Experimental procedure for elaboration of PDNS@TiO_2 hybrid DDS

2. Experimental Materials and Methods

2.1. Materials and reagents

Ethanol absolute was obtained from Tianjin Hengxing Chemical preparation. The ultrapure water used for solution preparation was prepared using Millipak filter of 0.22 µm pore size Millipore in Milli-Q system. Dopamine hydrochloride DA-HCl (~35-37%) was purchased from Aladdin Industrial Corporation. Sodium hydroxide (NaOH) (≥96%) and Boric acid (H_3BO_3) (≥ 99.5%) were purchased from Sinopharm Chemical Reagent. All chemical reagents were used as received without any purification. Hexa-fluoro ammonium titatante $(NH4)_2TiF_6$ (Analytical reagent) was obtained from Shanghai Macklin Biochemical Co. Ltd.

2.2. Characterization methods

Fourier transform infrared (FTIR) spectra were recorded on a Nicolet FT-IR 5700 spectrometer (USA) the samples were prepared using potassium bromide (KBr) pastille (few mg in 100mg of KBr)
UV-Visible absorption spectra were collected on Lambda 750S spectrophotometer (PerkinElmer, USA) with a scanning range from 200 to 900 nm. X-ray photoelectron spectroscopy (XPS) measurements were carried on an ESCALAB 250 XPS system (Thermo Electron Corporation, USA) with an Al Kα X-ray source (1486.6 eV photons), the analysis deep was of 8~10nm.UV-Vis absorption spectra were performed on a Lambda 750 spectrophotometer. Transmission electron microscope (TEM; Hitachi H-7650 microscope, operating at an accelerating voltage of 100 Kv) was used to determine the size of synthesised and modified PDNS and to evaluate the morphology of the nanoparticles. Zeta potential

analysis were carried out on Malvern Instruments Zetasizer Nano series instrument of samples (2.5 mg/mL in deionized water). These Characterisation were conducted at room temperature. NIR photothermal effect were studied on NIR laser diode (STPC-510P) purchased from Xiamen Black and Decker Intelligent Technology (diameter of the laser spot: ~8.0 mm). The temperature of solution was monitored using a digital thermometer with a thermocouple. Electron spin resonance spectra was recorded on Bruker ESR (A200S-95/12) at 25° C with microwave power of 32 mW and a microwave frequency of 9.42 GHz.

2.3. Preparation of experimental materials

2.3.1. Preparation of PDNS: PDA nanoparticles (PDNS) were prepared by the oxidation and self-polymerization of dopamine though previously reported methods [3] The PDNS with ~ 250 nm average diameter were prepared as follow: Briefly, 180 mg of dopamine hydrochloride (DA-HCl) was dissolved in 90 mL of deionized water, at T=50°C and under vigorous stirring, 760 µL of NaOH (1N) solution was added. After 5h, the obtained dark black solution were centrifuged (12500 rpm) and washed and then all high molecular weight materials were removed by 4500 rpm centrifugation.

2.3.2. Insitu deposition of TiO_2 on PDNS: In this step, the PDNS surface has been decorated with TiO_2 through liquid phase deposition method (LPD). First, 5mg of PDNS were ultrasonically dispersed in LPD solution for about 30 minutes, LPD solution is a mixture of 5 mL $(NH_4)_2TiF_6$ (0.1 M) as precursor and 5mL H_3BO_3 (0.2 M) prepared in high purity water. The plentifully active hydroxyl groups on PDA coating can chelate the Ti^{4+} metallic cations in $(NH_4)_2TiF_6$ in order to boost the nucleation and the growth of TiO_2 on the PDNS surface. Subsequently, the mixture container was sealed and placed in water bath under mild agitation at 40 °C for 2h in dark to graft TiO_2 then cooled down to room temperature. Finally the reaction products were centrifuged at 12300 rpm for 15 min and washed several times with diH_2O until a constant pH the reaction products was freeze dried for 8h.

2.3.3. The study of photothermal effect. To study the photothermal effect amount of PDNS@TiO_2 were dispersed in high purity water (1mL) at different concentrations (from 25 to 200 µg/mL)and then put into quartz specimen holder and then irrdiated with 808 nm NIR laser lat 2.5 W cm^{-2} for 10 min.The temperature of the solutions was measured through submerged thermocouple microprobe in the solution, the increase of temperature during 10 minutes of NIR irradiation should be recorded every 30s in ordre to skectch the temperature profiles of the irradiated samples. The photothermal test was repeated for three times independently. The mean value was recorded as the final result.

2.3.4. The study of ROS generation. Two samples of PDNS@TiO_2 was prepared for ESR measurement, one left in dark for 15 min, the other one left in dark then irradiated with UV (320 nm) for 5min just before ESR measurement. The ESR measurements were done without spin trap because according to literature PDA have a scavenging effect what makes it suitable spin adduct [13].

3. Results and Discussion

3.1. Morphological analysis

Transmission electron microscope images of synthesised PDNSs (see figure 2) indicates well spherical shaped nanoparticles of uniform appearance. The average particle size was determined to be size ~ 238.32 nm, after TiO_2 deposition the particle's size enhanced slightly to ~ 269.55 nm.

3.2. Structural Analysis

The successful synthesis of polydopamine nanoparticles and it modification with TiO_2 layer was further confirmed by FTIR spectroscopy and UV-Visible spectrophotometer.

3.2.1. FTIR: The spectrum of PDNS exhibits peaks at about 3276 cm^{-1} that proves the abundant hydroxyl groups of the PDA catechol groups, this peak become more broadened and shifted to 3397.9 cm^{-1} after the incorporation of TiO_2 with an hydroxyl ends as shown in FTIR spectra (figure 3a), the peak at 1688 cm^{-1} indicates the existence of a large amount of carbonyl groups (C=O) on surface of PDA. On other hand the peaks at 1557 cm^{-1} and 1618 cm^{-1} corresponding to the N–H and C=C aromatic ring stretching, respectively [14], while the peak at 842 cm^{-1} corresponds to C–N stretching.

3.2.2. UV-Vis: UV-vis spectra depicted in figure 3(b) of PDNS and PDNS@TiO_2 at concentration of 0.5mg/mL were compared. As shown in figure 3b PDNS absorb in UV-vis and NIR range. Generally the TiO_2 nanostructures have bandgap of >3.0 eV, which increases their absorbance in UV range and limits their absorption in the NIR light [1], in our case the TiO_2 nanostructures labelled PDNS have a considerable absorption in UV-Vis and NIR region, this could be explained by tuning absorbance of TiO_2 and PDNS consequently, an enhanced absorbance was remarked for PDNS@TiO_2 compared to PDNS. The UV-vis-NIR spectra shows three absorption peaks in UV range at 201, 250, 320nm characteristics of TiO_2 particles [15] in Visible and NIR range the two spectra are similar. The absorption of PDNS@TiO_2 is slightly higher than as synthesised PDNS.

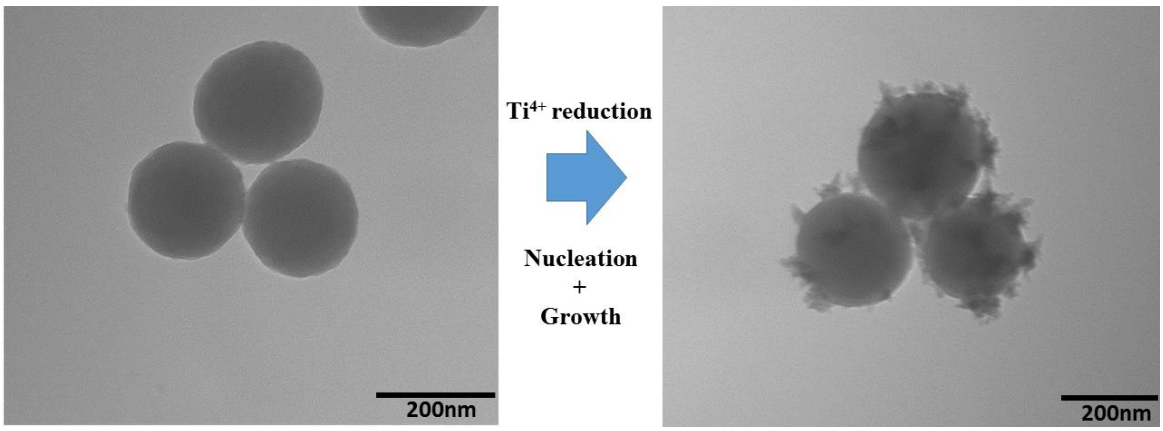


Figure 2. TEM images (scale 200 nm) of (a) as synthesised PDNS (b) PDNS@ TiO_2 after deposition

3.3. Surface chemistry

3.3.1. Zeta Potential: The zeta potential measurements illustrated in figure 3c reveal negatively charged PDNS surface(−32.4±2.533) due to the abundant hydroxyl and amine groups that tend to be negatively protonated above the isoelectric point (pH≥ 2, 3) [16]. After the formation of TiO_2 on the PDNS surface the zeta potential increased to −16.4±1.273 due to the absorption of high amount of Ti^{4+} cations, but it remains negative because a part of adsorbed Ti^{4+} have been reduced to TiO_2 with abundant hydroxyl groups on it.

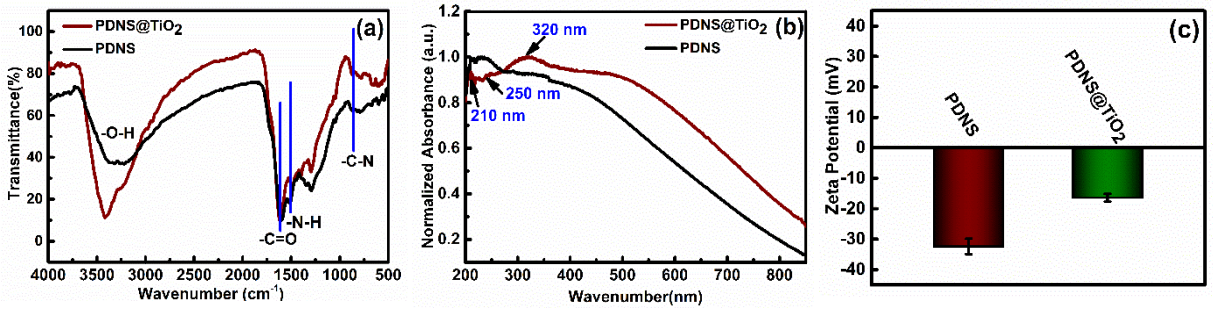


Figure 3. PDNS and PDNS@TiO_2 (a) FTIR spectra (b) UV-Vis spectra (c) Zeta potential

3.3.2. XPS: have been used for extraction of chemical surface information of unmodified and TiO_2 polydopamine, as shown in figure 4a the XPS survey spectra of three PDNS clearly show the peaks originated from C1s, O1s, and N1, while PDNS@TiO_2 shows four peaks originated from C1s, O1s, N1s and Ti2p. The high resolution C1s XPS spectra of PDNS in figure 4b was deconvoluted into four main peaks assigned to C-C/C-H (283.31 eV), C-N (284.36 eV), C-O (284.36 eV) and C=O (287.31 eV), respectively, the C=O appears due to oxidized form of PDA quinone group [2, 3, 17]. The XPS O1s and N1s spectra can further help to analyse the surface chemistry of the PDNS (figure 4c and 4g). N1s peaks in PDNS XPS spectra appeared at ~399.0 eV could be deconvoluted into three components; the peak at 398.0 eV assigned to -N= species of pyridine structure of PDA, the peak at 400 was attributed to the -N-H of the amine group in PDA cycle, last component at 402.61 eV corresponding to the primary amine-NH_2 and protonation primary amine $–NH^{+3}$ [2, 14]. O1s peaks in PDNS XPS spectra appeared at ~500.0 eV. The O 1s deconvoluted spectra of PDNS could be deconvoluted into four components C–O (531.3 eV), O–C O (532.3 eV), and C=O (533.1 eV), attributed to catechol groups of PDA (figure 4c). The C1s and the N1s deconvoluted spectra (see figure 4e and figure 4h) of the PDNS@TiO_2 are similar to that of PDNS just some change in component amount. However the O1s (figure 4f). High resolution spectra of PDNS@TiO_2 can be deconvoluted into 5 components (Ti-O-Ti at 528.68 eV) (Ti-OH at 529.38 eV), (O-C at 530.88 eV), (O=C at 530.14 eV), (O-H at 531.71 eV), and adsorbed O_2 (at 532.59 eV). [15] Ti high resolution XPS spectra in figure 4d shows two peaks at 457.10 and 463.33 eV, corresponding to Ti $2p_{3/2}$ (Ti^{4+}) and Ti $2p_{1/2}$ (Ti^{3+}), respectively revealing the reduction of a part of the Ti^{4+} into Ti^{3+} [1, 15].

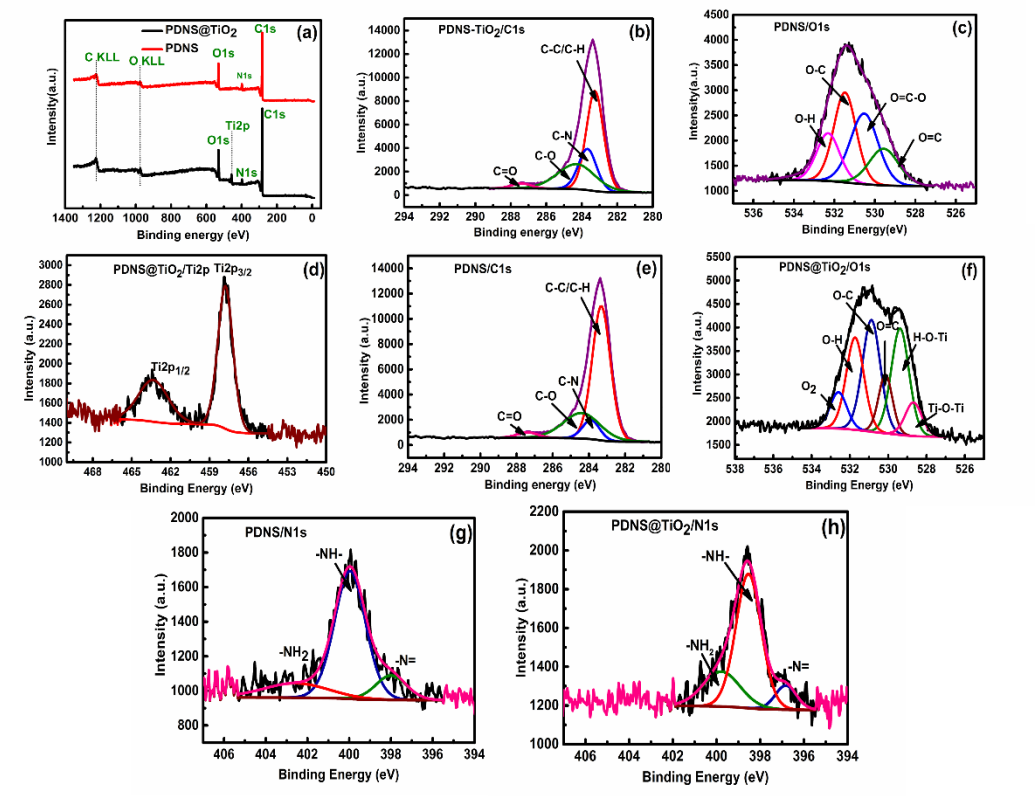


Figure 4. XPS data (a) XPS survey of PDNS and PDNS@TiO_2; (b) deconvoluted high resolution C1s spectra of PDNS powder (c) deconvoluted high resolution O1s spectra of PDNS powder; (d) deconvoluted high resolution Ti2p spectra of PDNS@TiO_2 powder; (e) deconvoluted high resolution C1s spectra of PDNS@TiO_2 powder (f) deconvoluted high resolution O1s spectra of PDNS@TiO_2powder; (g) deconvoluted high resolution C1s spectra of PDNS powder;(h) deconvoluted high resolution C1s spectra of PDNS powder

3.4. Photothermal measurements

In light of UV-Vis absorption spectra results, the PDNS and PDNS@TiO_2 can absorb in the NIR region (at 808 nm the absorbance of 200μg/mL was A_{808}=0.147). At different concentration PDNS@TiO_2, samples were irradiated with NIR laser (808nm) at power density of I=2.5 W/cm^2. The temperature profiles shows NIR induced temperature elevation dependence to nanostructure concentration as shown in figure 5a. The Temperature elevation records for PDNS@ TiO_2 were mainly attributed to the PDNS strong absorption and conversion of NIR light into heat. The photothermal conversion efficient (η) was calculated via equation (1), the heat capacity of solvent (Ultra-pure water) is ms Cs=4.2 J/°C. Maximum temperature elevation ΔT_{max}=29.8 was determined from heating curves (see figure 5b), whereas, the constant of time τ_s= 461.1s was determined from time plot (figure 5b) drawn using $t = -\tau_s \ln(\Delta T / \Delta T_{max})$ and cooling curve of 200 μg /mL PDNS@TiO_2 sample (figure5c). hS value (0.0091882 J/°C s) was extracted from $\tau_s = m_s C_s / hS$ and introduced in equation (1) along with other parameters, then η was calculated to be 34.9%, that slightly lower the PDA based nanostructures (40%) [18] due to the presence of TiO_2 that might limits the PDNS absorption of NIR light. However, our synthesised PDNS@TiO_2 nanostructures exhibits an efficient NIR to heat photothermal conversion enough for inducing sufficient hyperthermia.

$$\eta = \frac{hS\Delta T_{max} - Q_S}{I(1-10^{-A808})} \quad (1)$$

3.5. Generation of Reactive oxygen species

ESR spectra (figure 5d) of PDNS@TiO_2 show several paramagnetic peaks but with major differences in the peaks intensities, this could be caused by the presence of various paramagnetic species, the synthesis process, and the light effect, washing and drying during samples preparation for analysis and also the thermal effect during the storage.

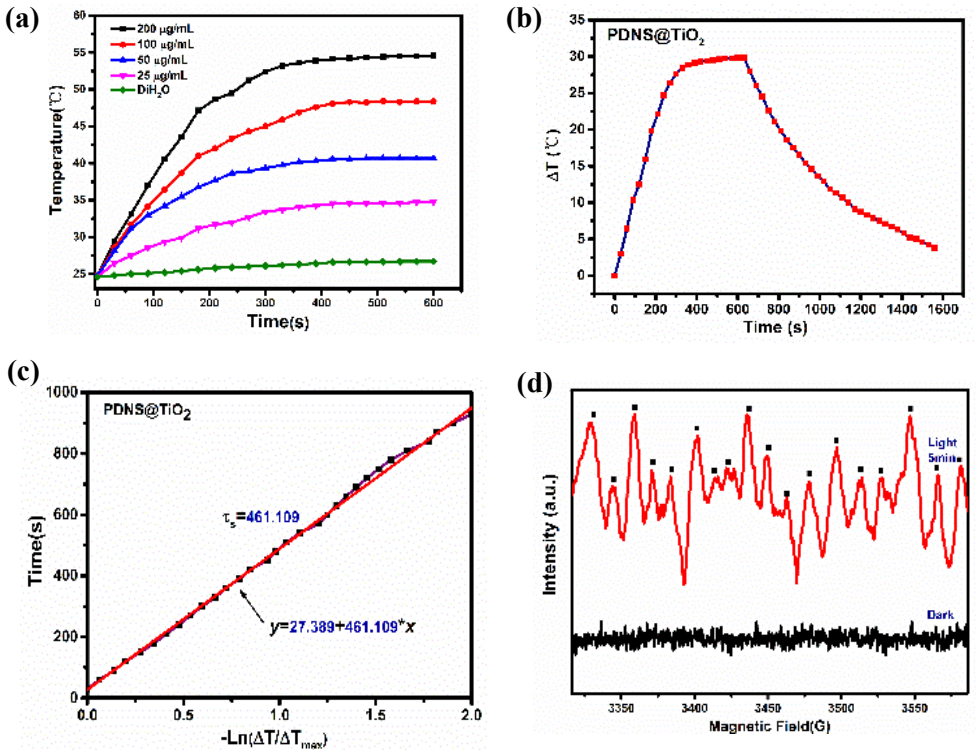


Figure 5. PDNS@TiO_2 (a) Temperature profiles at different concentration, (b) Heating cooling curve at 200 μg/mL, (c) Plot of cooling time versus negative natural logarithm of the temperature driving force, (d) ESR of generated ROS after PDNS@TiO_2 irradiation with UV.

On the other hand, the ESR spectra proves that the synthesised system generates ROS when it is photoxidized due to the presence of TiO_2 by using the polydopamine as spin trap agent that reacts with generated ROS and forms more stable radicals with half-life time longer enough for ESR analysis. The UV irradiated TiO_2 leads to PDA radical formation that has been detected by ESR [8]. The intensity of ESR signals depends to the concentration of free radicals. Our results proves the UV induced generation of toxic ROS using TiO_2 modified nanostructures.

4. Conclusion and future scope

Applying two therapeutically modality is primordial for enhanced treatment efficiency and decrease the side effects. The main objective of this work was to develop PDA based hybrid nanoparticles as UV and NIR photo absorbing agent. The results proved successful preparation of PDNS@TiO_2. The prepared PDNS@TiO_2 exhibit a good photothermal efficiency 34.9% due the PDNS substrate under NIR irradiation and also an effective generation of toxic ROS due to titanium metal oxide on the surface under UV irradiation. Our results further demonstrate that the as-obtained PDNS/TiO_2 nanostructures provides a synergetic NIR induced photothermal effect and UV induced ROS for photodynamic therapy application. A remarkable synergistic therapeutic effect has been achieved compared with respective single treatments. This work suggests that our synthesised nanoplatform could be applied in many filed such as biomedical and further photo-catalysis applications.

Acknowledgments

This work was financially supported by the National Natural Science Foundation of China (Grant No. 51673054), the Harbin City Science and Technology Innovation Talent Foundation (Grant No. 2017RAYXJ003), Shanghai Space Science and Technology Innovation Foundation (Grant No. SAST2017-114).

References

[1] Ou G, Li Z, Li D, Cheng L, Liu Z, Wu H.Photothermal therapy by using titanium oxide nanoparticles[J]. *Nano Research*, 2016, 29(5):1236-1243.

[2] Ye W, Chen Y, Zhou Y, Fu J, Wu W, Gao D, Zhou F, Wang C, Xue D.Enhancing the catalytic activity of flowerike pt nanocrystals using polydopamine functionalized graphene supports for methanol electrooxidation[J]. *Electrochimica Acta*, 2014, 142:18-24.

[3] Chen D, Zhao L, Hu W. Protein immobilization and fluorescence quenching on polydopamine thin films[J]. *Journal of Colloid & Interface Scienc*e, 2016, 477:123-130

[4] Ju KY, Lee Y, Lee S, Park SB, Lee JK. Bioinspired polymerization of dopamine to generate melanin-like nanoparticles having an excellent free-radical-scavenging property [J]. *Biomacromolecules,* 2011, *12*(3):625.

[5] Jiang Q, Luo Z, Men Y, Yang P, Peng H, Guo R, Tian Y, Pang Z, Yang W. Red blood cell membrane-camouflaged melanin nanoparticles for enhanced photothermal therapy[J]. *Biomaterials*, 2017,143:29-45.

[6] Rui Z, Sheng W, Ye T, Jiang X, Fu D, Shen S, Yang W, Polydopamine-coated magnetic composite particles with enhanced photothermal effect[J].*ACS Appl. Mater. Interfaces*, 2015,7:15876-84.

[7] Dong Z, Gong H, Gao M, Zhu W, Sun X, Feng L, Fu T, Li Y, Liu Z, Polydopamine nanoparticles as a versatile molecular loading platform to enable imaging-guided cancer combination therapy[J] *Theranostic*s, 2016, 6:1031-1042.

[8] He,W, Liu Y, Wamer WG, Yin JJ. Electron spin resonance spectroscopy for the study of nanomaterial-mediated generation of reactive oxygen species [J]. *Journal of Food and Drug Analysis*, 2014, 22(1):49-63

[9] Sun L, Li Z, Li Z, Hu Y, Chen C,Yang C, Du B, Sun Y, Besenbacher F, Yu M. Design and mechanism of core-shell TiO_2 nanoparticles as a high-performance photothermal agent[J], *Nanoscal*e, 2017, 9(42):16183-16192.

[10] Naserzadeh P, Ghanbary F, Ashtari P, Seydi E, Ashtari K, Akbari M. Biocompatibility assessment of titanium dioxide nanoparticles in mice feto-placental unit[J].*Journal of Biomedical Materials Research Part A*. 2017, 106(2):580–589.
[11] Kotagiri N, Sudlow GP, Akers WJ, Achilefu S.Breaking the depth dependency of phototherapy with cerenkov radiation and low-radiance-responsive nanophotosensitizers[J]. *Nature Nanotechnology*, 2015, 10(4):370-379.
[12] Zhang Y, Wang W, Ma X, Jia L. Polydopamine assisted fabrication of titanium oxide nanoparticles modified column for proteins separation by capillary electrochromatography[J]. *Analytical Biochemistry*, 2016, 512:103-109
[13] Ju, K. Y., Lee, Y., Lee, S., Park, S. B., & Lee, J. K. (2011). Bioinspired polymerization of dopamine to generate melanin-like nanoparticles having an excellent free-radical-scavenging property. *Biomacromolecules, 12*(3), 625-32.
[14] Han X, Zhang L, Li C. Preparation of polydopamine-functionalized graphene–Fe_3O_4 magnetic composites with high adsorption capacities[J]. *Rsc Advances*, 2014, 4(58):30536-30541.
[15] Su C, Liu L, Zhang M, Zhang Y, Shao C. Fabrication of Ag/TiO_2 nanoheterostructures with visible light photocatalytic function via a solvothermal approach[J]. *Crystengcomm*, 2012, 14(11):3989-3999.
[16] Su J, Sun H, Meng Q, Yin Q, Zhang P, Zhang Z, Yu H, Li Y. Long circulation red-blood-cell-mimetic nanoparticles with peptide-enhanced tumor penetration for simultaneously inhibiting growth and lung metastasis of breast cancer[J]. *Adv. Funct. Mater.* 2016, 26:1243-1252.
[17] Zangmeister RA, Morris TA, Tarlov MJ. Characterization of polydopamine thin films deposited at short times by autoxidation of dopamine[J]. *Langmuir,* 2013, 29:8619-8628.
[18] Jiang Q, Luo Z, Men Y, Yang P, Peng H, Guo R, Tian Y, Pang Z, Yang W, Red blood cell membrane-camouflaged melanin nanoparticles for enhanced photothermal therapy[J], *Biomaterials*, 2017, 143:29-45.